Report

Current Biology

Learning to perceive shape from temporal integration following late emergence from blindness

Highlights

- Recognizing objects moving through a narrow slit requires temporal integration
- We studied children that were blind throughout infancy, regaining sight years later
- With time and practice they learned to recover shape in slit-viewing conditions
- Complex visual inference routines can be acquired late despite early deprivation

Authors

Tanya Orlov, Maayan Raveh, Ayelet McKyton, Itay Ben-Zion, Ehud Zohary

Correspondence

udiz@mail.huji.ac.il

In brief

Orlov et al. study children that were effectively blind due to congenital cataract. Surgical treatment, years later, substantially improves their acuity. Amazingly, they also learn to recover object shape seen through a narrow slit. Thus, despite early visual deprivation, complex visual inference routines can be acquired well into adolescence.

Orlov et al., 2021, Current Biology *31*, 1–6
July 26, 2021
https://doi.org/10.1016/j.cub.2021.04.059

CellPress

Please cite this article in press as: Orlov et al., Learning to perceive shape from temporal integration following late emergence from blindness, Current Biology (2021), https://doi.org/10.1016/j.cub.2021.04.059

Current Biology

CellPress

Report

Learning to perceive shape from temporal integration following late emergence from blindness

Tanya Orlov,[1,2] Maayan Raveh,[1,2] Ayelet McKyton,[1,2] Itay Ben-Zion,[3] and Ehud Zohary[1,2,4,*]
[1]The Edmond and Lily Safra Center for Brain Sciences, The Hebrew University of Jerusalem, Jerusalem 91904, Israel
[2]Department of Neurobiology, The Alexander Silberman Institute of Life Sciences, The Hebrew University of Jerusalem, Jerusalem 91904, Israel
[3]Department of Ophthalmology, Padeh Medical Center, Poriya, Israel
[4]Lead contact
*Correspondence: udiz@mail.huji.ac.il
https://doi.org/10.1016/j.cub.2021.04.059

SUMMARY

Visual perception requires massive use of inference because the 3D structure of the world is not directly provided by the sensory input.[1] Particularly challenging is anorthoscopic vision—when an object moves behind a narrow slit such that only a tiny fraction of it is visible at any instant. Impressively, human observers correctly recognize objects in slit-viewing conditions by early childhood,[2,3] via temporal integration of the contours available in each sliver.[4,5] But can this capability be acquired if one has been effectively blind throughout childhood? We studied 23 Ethiopian children which had bilateral early-onset cataracts—resulting in extremely poor vision in infancy—and surgically treated only years later. We tested their anorthoscopic vision, precisely because it requires a cascade of demanding visual inference processes to perceive veridical shape. Failure to perform the task may allow mapping specific bottlenecks for late visual recovery. The patients' visual acuity typically improved substantially within 6 months post-surgery. Still, at this stage many were unable to recover shape under slit-viewing conditions, although they could infer the direction of global motion. However, when retested later, almost all patients could judge shape in slit-conditions necessitating temporal integration. This acquired capability often transferred to novel stimuli, in similar slit-viewing conditions. Thus, learning was not limited to the specific visual features of the original shapes. These results indicate that plasticity of sophisticated visual inference routines is preserved well into adolescence, and vision restoration after prolonged early-onset blindness is feasible to a greater extent than previously thought.

RESULTS AND DISCUSSION

We studied Ethiopian children suffering from early-onset complete bilateral cataracts that typically lasted many years. The vast majority of the children were found and surgically treated by our group. They were behaviorally tested months to years after the operation (for details, see Table S1). Shape temporal integration was assessed in two slit-viewing experiments using two groups of participants ("patients," 23 sight-retrieval patients, and "controls," 51 typically developing Ethiopian and Israeli children with normal or corrected vision).

In each trial of the first experiment (Figure 1A), a 2D shape moved behind a stationary slit. Next, the participants were presented with that shape and its flipped image (the foil), and were required to choose the shape they had just seen (see Method details, Experiment I for details). At the beginning of each run, the slit width was wider than the shape itself, such that the shape could be easily recognized. The slit width was adaptively changed using a staircase procedure to assess the recognition threshold (in slit width). The shapes were a cross-like image and its flipped version. Both stimuli were comprised of the same local elements (ellipsoids). Thus, when the slit width was small enough, discrimination between the target and the foil had to be based on temporal integration of the individual elements, recovering their global spatial structure.

A prerequisite for shape recovery using temporal integration in anorthoscopic conditions is a reliable assessment of the global motion because many possible shapes are consistent with the observed sequence of partial shape views.[4] To reconstruct the veridical shape, the spatial positions of the internally maintained shape views must be shifted according to the motion vector, so that these views could be combined with the currently visible portion of the shape.[4,5] We therefore also tested the participants' ability to judge the direction of motion in limiting slit-viewing conditions (in separate runs within the same day).

One concern is that the cataract-treated participants would perform poorly under slit-viewing conditions due to their relatively poor image resolution, even after surgery and its achieved optical correction.[6,7] The patients' visual acuity typically improved dramatically in the first 6 months after surgery, but it never reached the level of their normally developing peers[6] (Figures S1A–S1C; Table S1). To account for this difference, our

Please cite this article in press as: Orlov et al., Learning to perceive shape from temporal integration following late emergence from blindness, Current Biology (2021), https://doi.org/10.1016/j.cub.2021.04.059

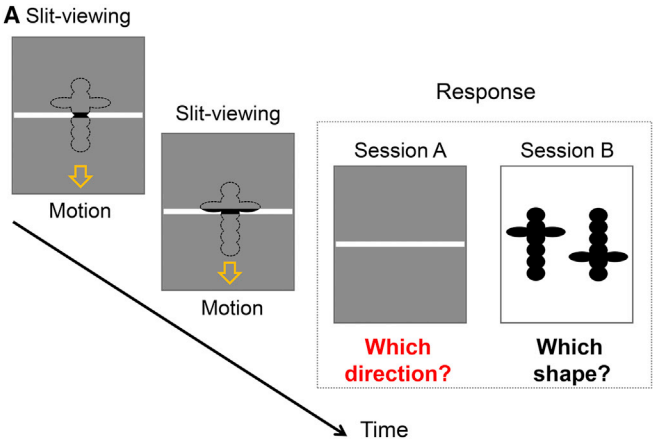

Figure 1. Shape temporal integration in late cataract-treated individuals: Experimental design

(A) A cross-like shape moved at a fixed speed in a direction orthogonal to the slit orientation, such that only a portion of the shape was visible at any instant (marked in black, dashed outlines for shapes are for visualization purposes only). After the shape completed its motion, the task was either to report the direction of slit-viewed motion (e.g., up or down for horizontal-slit trials) or the object's shape (e.g., choosing either the left or right shape presented in the test panel). The two tasks were performed in separate blocks. The same procedure was repeated using a vertical slit. Slit width was adaptively changed using a staircase procedure to assess the direction/shape discrimination threshold.

(B) Control participants were presented with a low-pass filtered version of the stimuli to control for the patients' poor visual acuity.

See also Figure S1.

control participants were shown a lowpass filtered version of the original images: all spatial frequencies above 1 cycle per degree (cpd) were filtered out, introducing image blur greater than that experienced by the patient with the *poorest* visual acuity at the time of testing (Figures 1B and S1D).

We conducted the experiment using both horizontal and vertical slit configurations. Figure 2 shows the group-mean thresholds for motion (red) and shape (black) discrimination in the patients (filled bars) and controls (empty bars) under horizontal-slit (A) and vertical-slit (B) conditions. Importantly, both groups were able to judge the direction of global motion even when the slit width consisted of a tiny fraction of the full object. However, the patients were much poorer than the controls in the cross-shape recognition task. The patients' performance in this task was correlated with their post-operative acuity (but not with their pre-operative acuity or age at surgery; Figures S2A–S2D).

An ANOVA on the performance scores with task (direction, shape), slit orientation (horizontal, vertical), and the group identity (patients, controls) as factors revealed a significant task × group interaction term indicating that the patients indeed differed from the controls in their ability to recognize slit-viewed shapes, regardless of slit orientation ($F(1,26) = 26.1$, $\eta_p^2 = 0.501$, $p < 0.001$; see also Quantification and statistical analysis, Statistics). Follow-up t tests confirmed that shape-recognition thresholds were higher for the patients than the controls (horizontal and vertical slit: $t(26) = 4.70$ and 5.18, respectively; $p < 0.001$ for both), while no such difference was found in the motion direction task ($t(26) = -1.31$ and 1.01; $p = 0.200$ and 0.322, respectively).

Importantly, if the slit was wide enough to simultaneously observe the three short arms of the cross shape (see insets in Figures 2A and 2B, left), discrimination between the slit-viewed shape and its flipped version could be done without temporal integration. We therefore identified the critical slit width (26.6% of the shape length; green dashed line) as a critical criterion for temporal integration: below this value, temporal integration must be used to recover shape. As Figures 2A and 2B show, on average, the patients' performance in the shape task was poor, around the critical value (indeed, the patients' thresholds did not differ significantly from this criterion; Figure S2B). The controls, on the other hand, were far better, because they effectively utilized temporal integration to solve the problem.

Clearly, many patients failed to use temporal integration for shape recovery in anorthoscopic conditions. But can this capability be acquired with repeated practice on the task? Figure 2C presents the individual shape-recognition thresholds of a subgroup of 11 patients that were tested in multiple sessions, days or many months apart. Each individual's vertical- and horizontal-slit thresholds were averaged to get a more reliable performance estimate.

In their initial test (dark-gray diamonds) after an average of 89 slit-viewing trials (range 71–96; SD = 11 trials), 6/11 of the patients had a shape-recognition threshold above the critical criterion, so that the patients' group performance was not significantly different from this critical value ($t(10) = 0.72$, $p = 0.488$). In contrast, all but one of the 36 control participants (tested under both slit orientations) passed this criterion (see X's in Figure 2C; $t(35) = -13.2$, $p < 0.001$) so that there was a highly significant difference between the groups ($t(45) = 6.8$, $p < 0.001$).

But the patients showed significant improvement in their performance in their subsequent tests a year later (light-blue diamonds in Figure 2C) or even a few days after the initial testing (dark-blue diamonds; see also Figure S2E). To quantify the effect, we applied a linear mixed model, with test repetition (the 1st, 2nd, and 3rd test) as the factor of interest. Visual acuity was added as a covariate. The repetition factor had a significant effect ($F(2,23) = 8.2$, $p = 0.002$). Follow-up t test confirmed that performance got better with practice (the 1st versus 3rd test: $t(10) = 5.8$, $p < 0.001$, Cohen's $d = 1.74$). Crucially, at the last test, after 210 slit-viewing trials (range 107–276; SD = 66 trials) the shape-recognition threshold of all patients except one (10/11) was below the critical value ($t(10) = -3.7$, $p = 0.004$). This suggests that sight-recovery patients learn to apply temporal integration to recognize shape in anorthoscopic conditions. Accordingly, the difference in the task performance between the patients and controls disappeared ($t(13) = 0.98$, $p = 0.345$; degrees of freedom were adjusted from 45 to 13 as Levene's

Please cite this article in press as: Orlov et al., Learning to perceive shape from temporal integration following late emergence from blindness, Current Biology (2021), https://doi.org/10.1016/j.cub.2021.04.059

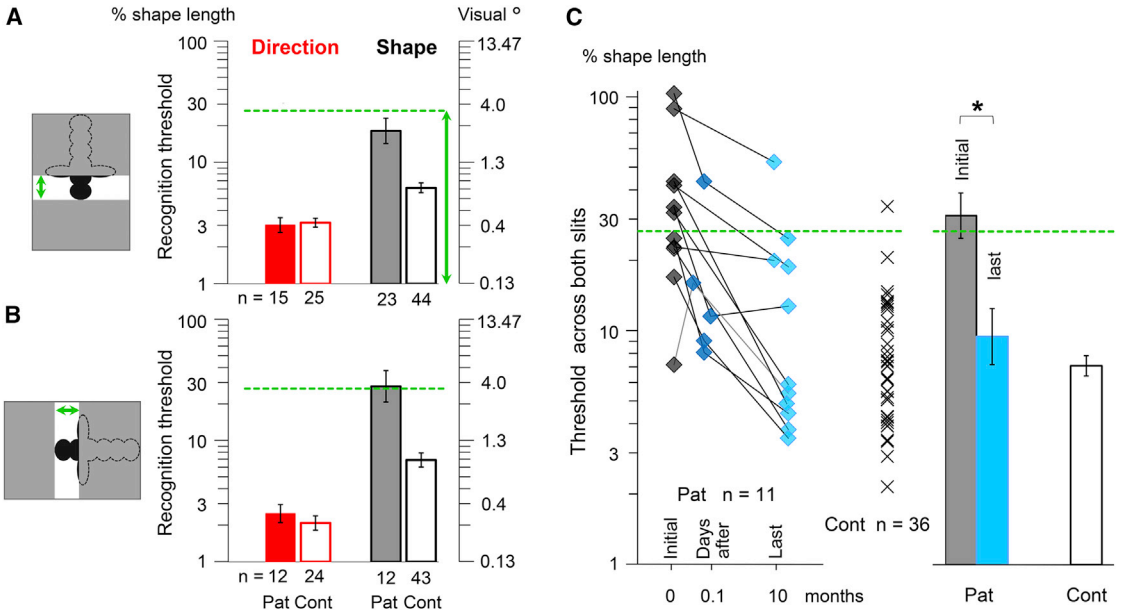

Figure 2. Shape temporal integration in late cataract-treated individuals: Results

(A and B) Group-mean slit-width thresholds for the motion direction (red) and shape (black) tasks, under horizontal-slit (A) and vertical-slit (B) viewing, in the newly sighted (Pat, filled bars) and controls (Cont, empty bars). The thresholds were calculated as percent (%) of the full shape length (left y axis); the corresponding size in visual angle (at 40 cm viewing distance) is shown on the right y axis. Data are represented as mean ± SEM (using a log scale). Note that if the slit was wide enough to simultaneously observe the three short arms of the cross shape (e.g., the horizontal part of the cross along with its short vertical end element; see insets on the left), the cross-shape task could have been recovered without any temporal integration. This defines a critical criterion for shape integration (26.6% of the shape length; green dashed line). Below this critical value, temporal integration is required to solve the task.

(C) Individual shape recognition thresholds (averaged across the horizontal- and vertical-slit runs) of controls (Cont, X's) and the newly sighted (Pat) in their initial test (dark-gray diamonds), after a few days (dark-blue diamonds), and about a year later (light-blue diamonds). Bars denote corresponding group-mean thresholds (mean ± SEM using a log scale) of controls (empty bar) and the newly sighted in their initial (filled gray bar) and last (filled blue bar) test. A significant improvement in the performance between the initial and the last test is denoted by an asterisk ($p < 0.001$).

See also Figure S2 and Table S1.

test indicated unequal variances: $F = 6.8$, $p = 0.012$). Note that while performance in the initial test was superior in patients with better visual acuity (Figure S2B), the repetition-number effect was independent of acuity (since the variance accounted for by visual acuity was regressed out; see also Figure S2F).

Did the patients merely learn to solve a *specific* problem, taking advantage of the fact that the same stimulus appeared throughout the experimental session (see Method details, Experiment I for an example strategy)? A litmus test for a true, newly acquired capability is that it is generalized, allowing recovery of *any* shape, in similar slit-viewing conditions. To verify this, we conducted a second shape discrimination experiment, similar to the previous one, now using 48 unique shapes, organized into 24 pairs (Figure 3A; Method details, Experiment II). Each shape pair was generated such that the characteristic *local* visual features (i.e., contour curvature) were highly similar between the two shapes. Crucially, during the whole session, each image was shown traversing across the slit only once. Thus, the patients could not learn to focus on specific visual features to solve the unique-shapes task.

Use of trial-unique stimuli solved the problem of stimulus-specific learning but resulted in substantial variation in the critical slit width for the different shapes. The critical slit width, below which temporal integration was compulsory for shape recovery, varied between pairs from 25.0% to 38.9% of the full image (mean = 30.4%, SD = 4.5%; see examples in Figure 3B and Method details, Experiment II). To control for this variation, we calculated the normalized slit width for each trial in the staircase, considering the specific shape viewed on that trial. Specifically, the slit width of the trial was divided by the corresponding critical slit width for that shape, and the log of their ratio was used as the normalized slit-width value (see the normalized data of one exemplary case in Figure 4A). Then, each individual's recognition threshold was assessed by computing the average normalized slit width across the final six reversals (arrows in Figure 4A; the patient's raw staircase data are shown in Figure S3A). A normalized recognition threshold below zero, as in this exemplary patient, indicates compulsory use of temporal integration for shape recovery. The results of all patients in the unique-shapes test are shown in Figure 4B, as a function of their performance in the cross-shape test. Note the positive correlation between the two measures ($r(19) = 0.62$; $p = 0.003$).

The normalized threshold of a third of the patients (7/21) in the unique-shapes task was below zero (see Figures S3A–S3G for the individual staircase plots). Thus, these seven patients were necessarily using a temporal integration strategy. The shape-recognition thresholds of about a quarter of the patients (5/21) were worse than the critical value in both (cross-shape and unique-shapes) tests, demonstrating a total failure in strategy acquisition. The rest (9/21) performed well only in the

Please cite this article in press as: Orlov et al., Learning to perceive shape from temporal integration following late emergence from blindness, Current Biology (2021), https://doi.org/10.1016/j.cub.2021.04.059

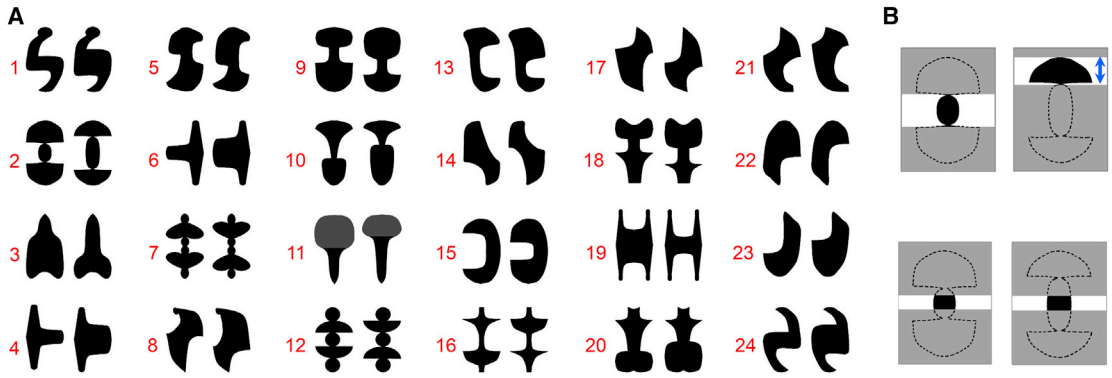

Figure 3. Studying learning generalization using the unique-shapes task

(A) The image set used in this control experiment consisted of 48 stimuli organized into 24 pairs. Each image was shown once traversing behind the horizontal slit, and the participant had to choose that image later, when shown together with its paired foil image.

(B) Examples of two images from a pair (#2). The critical slit-width value (defined per pair) was the smallest slit size, which allowed discrimination between the two images based on a specific *local* feature (e.g., the "mushroom head" size, critical value indicated by arrow in the upper right).

See also Method details, Experiment II and Figure S3.

cross-shape test (their recognition thresholds were better than the critical value in this test, but not in the unique-shapes test; see an example in Figure S3H). One might conclude that these patients failed to use temporal integration and solved the cross-shape task using a stimulus-specific strategy. However, the unique-shapes task is much more difficult due to the variation in shapes across trials, thus inducing a greater load on sensory memory. Indeed, none of the patients succeeded in the unique-shapes task without doing so in the cross-shape task. It is therefore more likely that the sub-group who performed well only with cross-like shapes was actually capable of integrating shape slivers over time, but only when the slivers were easy to remember due to their repeated appearance.

The strongest piece of evidence suggesting that the patients were using temporal integration in both tests is that patients with previous experience in the cross-shape task typically did better in the unique-shapes test ("practiced" subgroup; Figure 4B, red filled circles) than the ones that had done both tests for the first time on the same day ("naive" subgroup, empty circles). Indeed, the majority (6/7) of the individuals who were successful in the unique-shapes test had previous experience with the cross-shape task. Note that the "practiced" subgroup was *not* better than the "naive" subgroup, *a priori*, due to sheer coincidence (see details in Quantification and statistical analysis, Experiment II). Thus, the gains of previous practice typically generalized to novel stimulus conditions. A between-groups ANOVA corroborated this, showing that the effect of previous practice (practiced, naive) on the unique-shapes scores was significant ($F(1,17) = 8.1$, $\eta_p^2 = 0.323$, $p = 0.011$) after regressing out the effects due to the (current) visual acuity and time since surgery (by using these variables as covariates; see also Figure S3K). Collectively, the above results suggest that there was a transfer of learning from the cross-shape task to the unique-shapes task, regardless of the patients' visual acuity and time since surgery. Our data therefore indicate that newly sighted patients can learn to utilize temporal integration to recover shape in anorthoscopic conditions.

A comparison of the newly sighted capabilities in "dorsal" (motion) versus "ventral" (shape) tasks offers some important insights. The children's global-motion assessment was as good as their normally developing peers already at the first testing. Possibly, this function rapidly recovered soon after surgery (as in Mansouri and Hess,[8] but see Ellemberg et al.[9] and Hadad et al.[10]), similar to the ability to judge color and size[11,12] and finer spatial frequencies.[13] Likewise, our patients had no problem matching simple full-viewed 2D shapes (as in McKyton et al. [11] and Ostrovsky et al.[14,15]). This may well be due to an enhancement of visual capabilities that were available, to a very limited extent, before surgery. These findings resemble the results from the study of patient MM, who became fully blind at age 3 and regained vision at age 46.[16,17] Although MM could recognize simple 2D shapes shortly after surgery, he failed to recognize static 3D objects. In contrast, he readily identified the direction of complex plaid motion (which requires the solution of the aperture problem, as in our case[4]), and could recognize 3D objects when rotated around their axis. Furthermore, a case study of a few late cataract-treated patients suggested that motion information enables the development of scene-parsing skills after surgery, despite the patients' prolonged early-onset blindness.[14] Together, our current data and these results suggest that the motion-processing pathways are likely to be more resilient to long-term visual deprivation than the form-processing pathways.[18]

In our dynamic slit-viewing conditions, shape recovery could only be carried out after the global-motion vector was extracted.[4] Shape information was not only extremely limited at any moment, but the observed fragments also overlapped in retinotopic space. Obviously, sufficient spatial and temporal resolution (to measure contours within each shape-sliver[19] and segregate the individual slivers in time[20]), convergence of information from both ventral and dorsal pathways, and an interaction with non-retinotopic sensory memory[4,5,21] were necessary for the job. Remarkably, despite this computational complexity, the newly sighted improved dramatically in our shape-inference task.

Both the learning effect (Figure 2C) and the degree of generalization to novel stimuli (Figure 4B) were independent of the patients' visual acuity at the time of testing. This should not be

Please cite this article in press as: Orlov et al., Learning to perceive shape from temporal integration following late emergence from blindness, Current Biology (2021), https://doi.org/10.1016/j.cub.2021.04.059

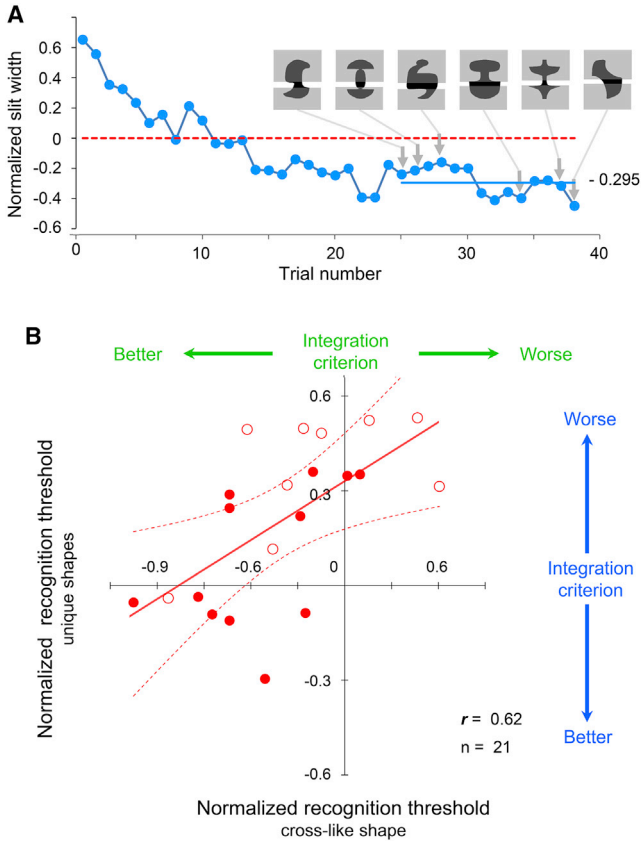

Figure 4. Behavioral performance in the unique-shapes task

(A) Performance of an exemplary patient, showing the normalized slit width as a function of the trial number in the session. The slit width of each trial was normalized by the corresponding critical integration value for the slit-viewed shape (in that trial) by taking the log of their ratio. The individual's recognition threshold (−0.295; denoted by the blue horizontal line) was assessed by computing the average across the final six reversals (denoted by gray arrows; the patient's raw staircase data are shown in Figure S3A). A value below zero indicates that the slit width on that trial was smaller than the critical value, necessitating temporal integration. The inset shows specific slit-viewed images shown in the reversal trials.

(B) Scatterplot showing individual performance in the unique-shapes task as a function of performance in the cross-shape task. In both tasks (performed under the same horizontal-slit orientation), the individual's recognition threshold was normalized (in the unique-shape task, as explained in A; in the cross-shape task, by taking the log of the ratio between the individual's recognition threshold and the critical slit width for that task). Negative values are cases in which the threshold was lower than the critical slit width, necessitating temporal integration. When the cross-shape test was performed multiple times (Figure 2C), the result of the most recent test was used in the analysis. Filled red circles indicate cases in which the participants performed the cross-shape test in the past (3–6 times, under different slit orientations), while empty circles are cases when both the cross-like and unique-shapes tests were novel. The scatter diagram (of all data points) is fitted with a regression line and the associated 95% confidence intervals.

See also Figure S3 and Table S1.

mistaken as evidence that visual acuity is irrelevant. Clearly, a minimal level of visual acuity is required to reliably recognize image contours, and achieving this threshold acuity can open a window for learning new visual routines[22] including sophisticated spatiotemporal integration. However, above this level, the acuity is likely to have only marginal effects, and the bottleneck for further improvement in the task might be set by other factors (e.g., limited sensory memory or problems in the binding of motion and shape information). The visual acuity of the newly sighted increased almost 6-fold between surgery and the initial cross-shape test (geometric average pre-op: 0.6 cpd, range: [0.06–2.56]; post-op, initial test: geometric mean, 3.5 cpd, range, [1.2–9.6]). Thus, in all likelihood, they attained the required visual acuity for the task prior to the initial testing (indeed, the controls were able to perform the task despite greater image blur, using lowpass filtering at 1 cpd). On the other hand, the patients' acuity did not substantially improve further between the initial and the last test (geometric mean, 3.7 cpd, range, [0.9–14.6]). Thus, learning could not have been due simply to a better quality of the visual input (e.g., availability of finer contours). At that stage, performance was probably determined to a larger extent by the level of implicit understanding of how to process the temporally fragmented information using sophisticated integration in non-retinal coordinates.

We did not find clear evidence for an effect of the age at surgery on task performance. However, most of our patients were surgically treated at late childhood/early adolescence. We therefore cannot exclude that surgery at a later stage (and/or the related deprivation duration) may have a deleterious effect on the chances for full vision recovery. Indeed, MM's older age at surgery, well after reaching adulthood, and his poor visual acuity (i.e., 1.2 cpd even ~10 years after sight restoration) probably precluded the development of proper visual object recognition.[16,17] The visual cortex of our patients is likely to be more plastic than that of MM due to their relatively young age.

In summary, we show conclusively that following surgery, the newly sighted learned to recognize shapes when these could only be recovered using both temporal integration and other complex mapping routines. Thus, amazingly, even in extreme, anorthosopic conditions, shape integration is attainable despite years of visual deprivation lasting far beyond the typical age of trait acquisition.[2,3,19,23] This sophisticated spatiotemporal integration capability can probably emerge only (1) if visual acuity is better than the limiting threshold, allowing the person to reliably recover image contours, (2) with enough practice, and (3) if there is sufficient plasticity of the visual system to optimally shape the neural circuits underlying the relevant computation.

STAR★METHODS

Detailed methods are provided in the online version of this paper and include the following:

- KEY RESOURCES TABLE
- RESOURCE AVAILABILITY
  - Lead Contact
  - Materials Availability
  - Data and Code Availability
- EXPERIMENTAL MODEL AND SUBJECT DETAILS
  - Participants
  - Inclusion tests
- METHOD DETAILS
  - Experiment I
  - Experiment II

SUPPLEMENTAL INFORMATION

Supplemental information can be found online at https://doi.org/10.1016/j.cub.2021.04.059.

ACKNOWLEDGMENTS

We thank all the children that participated in our tests. Thanks to Ilana Nave, Asael Sklar, and Yuval Porat for their comments on the manuscript, and Diana Moroshek, Yuval Porat, and Lior Aloni for their help in running the experiments. This study was supported by the DFG German-Israeli Project Cooperation grant #Z0 349/1 and the Israel Science Foundation grant 473/18 to E.Z. Finally, we wish to thank the local team including Zemene Zeleke for taking care of all logistics, and Drs. Helen Sisay and Demoze Arega for clinical care and surgical treatment of the patients.

AUTHOR CONTRIBUTIONS

T.O. and E.Z. conceived and designed the experiments together. M.R., A.M., T.O., and E.Z. collected the data. T.O. analyzed the data. T.O. and E.Z. wrote the manuscript. I.B.-Z. was the pediatric ophthalmologist responsible for all clinical aspects, including medical and optometric examinations, and surgeries. He supervised the work of the local Ethiopian crew during the surgeries.

DECLARATION OF INTERESTS

The authors declare no competing interests.

Received: June 11, 2020
Revised: March 8, 2021
Accepted: April 26, 2021
Published: May 26, 2021

REFERENCES

1. Marr, D. (1982). Vision (Freeman).
2. Imura, T., and Shirai, N. (2014). Early development of dynamic shape perception under slit-viewing conditions. Perception *43*, 654–662.
3. Skouteris, H., and McKenzie, B.E. (1997). Recognition of form by pre-school children after progressive visual exposure. Early Dev. Parent. *6*, 159–170.
4. Shimojo, S., and Richards, W. (1986). "Seeing" shapes that are almost totally occluded: a new look at Parks's camel. Percept. Psychophys. *39*, 418–426.
5. Palmer, E.M., Kellman, P.J., and Shipley, T.F. (2006). A theory of dynamic occluded and illusory object perception. J. Exp. Psychol. Gen. *135*, 513–541.
6. Kalia, A., Lesmes, L.A., Dorr, M., Gandhi, T., Chatterjee, G., Ganesh, S., Bex, P.J., and Sinha, P. (2014). Development of pattern vision following early and extended blindness. Proc. Natl. Acad. Sci. USA *111*, 2035–2039.
7. Ellemberg, D., Lewis, T.L., Maurer, D., Lui, C.H., and Brent, H.P. (1999). Spatial and temporal vision in patients treated for bilateral congenital cataracts. Vision Res. *39*, 3480–3489.
8. Mansouri, B., and Hess, R.F. (2006). The global processing deficit in amblyopia involves noise segregation. Vision Res. *46*, 4104–4117.
9. Ellemberg, D., Lewis, T.L., Maurer, D., Brar, S., and Brent, H.P. (2002). Better perception of global motion after monocular than after binocular deprivation. Vision Res. *42*, 169–179.
10. Hadad, B.S., Maurer, D., and Lewis, T.L. (2012). Sparing of sensitivity to biological motion but not of global motion after early visual deprivation. Dev. Sci. *15*, 474–481.
11. McKyton, A., Ben-Zion, I., Doron, R., and Zohary, E. (2015). The limits of shape recognition following late emergence from blindness. Curr. Biol. *25*, 2373–2378.
12. Andres, E., McKyton, A., Ben-Zion, I., and Zohary, E. (2017). Size constancy following long-term visual deprivation. Curr. Biol. *27*, R696–R697.
13. Maurer, D., Mondloch, C.J., and Lewis, T.L. (2007). Effects of early visual deprivation on perceptual and cognitive development. Prog. Brain Res. *164*, 87–104.
14. Ostrovsky, Y., Meyers, E., Ganesh, S., Mathur, U., and Sinha, P. (2009). Visual parsing after recovery from blindness. Psychol. Sci. *20*, 1484–1491.
15. Ostrovsky, Y., Andalman, A., and Sinha, P. (2006). Vision following extended congenital blindness. Psychol. Sci. *17*, 1009–1014.
16. Huber, E., Webster, J.M., Brewer, A.A., MacLeod, D.I., Wandell, B.A., Boynton, G.M., Wade, A.R., and Fine, I. (2015). A lack of experience-dependent plasticity after more than a decade of recovered sight. Psychol. Sci. *26*, 393–401.
17. Fine, I., Wade, A.R., Brewer, A.A., May, M.G., Goodman, D.F., Boynton, G.M., Wandell, B.A., and MacLeod, D.I. (2003). Long-term deprivation affects visual perception and cortex. Nat. Neurosci. *6*, 915–916.
18. Braddick, O., and Atkinson, J. (2011). Development of human visual function. Vision Res. *51*, 1588–1609.
19. Kiorpes, L. (2016). The puzzle of visual development: behavior and neural limits. J. Neurosci. *36*, 11384–11393.
20. Wutz, A., Muschter, E., van Koningsbruggen, M.G., Weisz, N., and Melcher, D. (2016). Temporal integration windows in neural processing and perception aligned to saccadic eye movements. Curr. Biol. *26*, 1659–1668.
21. Öğmen, H., and Herzog, M.H. (2016). A new conceptualization of human visual sensory-memory. Front. Psychol. *7*, 830.
22. Ullman, S. (1984). Visual routines. Cognition *18*, 97–159.
23. Lewis, T.L., Ellemberg, D., Maurer, D., Dirks, M., Wilkinson, F., and Wilson, H.R. (2004). A window on the normal development of sensitivity to global form in glass patterns. Perception *33*, 409–418.
24. Brainard, D.H. (1997). The psychophysics toolbox. Spat. Vis. *10*, 433–436.
25. Chung, S.T., and Legge, G.E. (2016). Comparing the shape of contrast sensitivity functions for normal and low vision. Invest. Ophthalmol. Vis. Sci. *57*, 198–207.
26. World Health Organization (2018). International classification of diseases for mortality and morbidity statistics, 11th Revision (World Health Organization).
27. Levitt, H. (1971). Transformed up-down methods in psychoacoustics. J. Acoust. Soc. Am. *49*, 2–, 467.
28. Attneave, F. (1954). Some informational aspects of visual perception. Psychol. Rev. *61*, 183–193.
29. Feldman, J., and Singh, M. (2005). Information along contours and object boundaries. Psychol. Rev. *112*, 243–252.
30. Norman, J.F., Phillips, F., and Ross, H.E. (2001). Information concentration along the boundary contours of naturally shaped solid objects. Perception *30*, 1285–1294.
31. Lesmes, L.A., Lu, Z.L., Baek, J., and Albright, T.D. (2010). Bayesian adaptive estimation of the contrast sensitivity function: the quick CSF method. J. Vis. *10*, 1–21.
32. Karni, A., and Sagi, D. (1993). The time course of learning a visual skill. Nature *365*, 250–252.

Please cite this article in press as: Orlov et al., Learning to perceive shape from temporal integration following late emergence from blindness, Current Biology (2021), https://doi.org/10.1016/j.cub.2021.04.059

CellPress

STAR★METHODS

KEY RESOURCES TABLE

REAGENT or RESOURCE	SOURCE	IDENTIFIER
Deposited data		
Datasets	This paper; Mendeley Data	https://doi.org/10.17632/57ry7yds8h.1
Software and algorithms		
MATLAB R2019b	MathWorks	https://www.mathworks.com/
Psychtoolbox 3.0.10	[24]	https://www.psychtoolbox.org/
SPSS Version 26.0.0.0	IBM	http://www.ibm.com/analytics/spss-statistics-software
Other		
Presentation 22	Neurobehavioral Systems	http://www.neurobs.com/

RESOURCE AVAILABILITY

Lead Contact

Further information for resources should be directed and will be fulfilled by the Lead Contact, Ehud Zohary (udiz@mail.huji.ac.il).

Materials Availability

This study did not generate new unique reagents.

Data and Code Availability

Full dataset including all the experimental results of the participants in this paper is available (Mendeley Data DOI: https://doi.org/10.17632/57ry7yds8h.1). This study used standard, custom-built MATLAB programmed scripts that will be available from the Lead Contact upon request.

EXPERIMENTAL MODEL AND SUBJECT DETAILS

Participants

Twenty-three Ethiopian children with early-onset bilateral cataracts (11 girls and 12 boys; ages 8.2 - 19.9 years [at the first test], mean age = 12.3 years, SD = 3.0) fulfilled our inclusion criteria and participated in the experiments (Table S1). Their dense bilateral cataracts were most likely congenital or developed within a few months after birth, as all had clear nystagmus, a classical sign of early-onset blindness. The patients were presumably blind from birth, according to written reports at their entry to the blind school and/or oral statements by their parents. Almost all of them (22/23) attend (or attended in the past) blind schools, and learn via Braille (or other non-visual media). Pre-surgical ophthalmological examination showed that they had extremely poor pattern vision: typically, limited to light or hand motion perception and, at most, finger counting from close range. We assessed pre-surgical visual acuity (in terms of the cutoff spatial frequency, cpd) of 19 (out of 23) patients using our tests, developed for children with severe visual disabilities (see McKyton et al.[11] and Method details, Contrast sensitivity assessment for the tests' details). The acuity scores were also converted to the Snellen scale and log of minimum angle of resolution (logMAR[25]) for better comparison with other studies (Table S1). The patients' average pre-op logMAR was 1.7 (corresponding to a geometric average of pre-op spatial frequency of 0.6 cpd). 12/19 had logMAR > 1.3, equivalent to a visual acuity worse than 3/60 (20/400) on the Snellen scale (i.e., blind by W.H.O standards[26]). 7/19 had an acuity (1.3 > logMAR > 1.0), worse than 6/60 (i.e., 20/200, the standard definition of legal blindness in the U.S.) indicating a severe impairment of vision.

Lack of earlier diagnosis and/or local resources/facilities prevented these children from receiving early treatment. They were diagnosed by our team through an active screening effort, and consequently had a cataract-removal surgery in both eyes at late childhood (mean age = 10.3 years, SD = 3.7) at Hawassa Referral Hospital. All but one had an intraocular lenses implantation. One patient (#p11) was operated at one year of age (not by our team), without implantation of artificial lenses (due to early age). He was not wearing corrective glasses when we first met him at age 12.5. We prescribed him glasses, and he participated in our first slit-viewing experiment.

The children's guardians gave their written consent for the operation and for participating in the behavioral testing. The children performed the tests in Hawassa Referral Hospital or in their blind schools (Shashemene, Bako, Wolaita and Sebeta Blind Schools)

Please cite this article in press as: Orlov et al., Learning to perceive shape from temporal integration following late emergence from blindness, Current Biology (2021), https://doi.org/10.1016/j.cub.2021.04.059

4.4 months to 12.7 years after the operation. The procedures were approved by the ethics committee of the Hebrew University of Jerusalem and Hawassa University. For more information regarding the newly-sighted participants, see Table S1.

Fifty-one typically developing Ethiopian and Israeli children with normal or corrected vision (26 Ethiopian and 25 Israeli children; 14 girls and 37 boys; ages 7.8 – 15.0 years; mean age = 11.4 years, SD = 2.1) served as control participants in the slit-viewing experiments. The children's guardians gave their written consent for participating in the behavioral testing.

Inclusion tests

The slit-viewing experiments required comprehension of the concept of a shape moving behind a slit. To assure that the patient had the basic capabilities to perform this task, a number of slit-viewing familiarization trials (with the slit width equal to 160% of the shape length, at either slit orientation) were presented. The participant had to have at least four consecutive correct judgments of the direction of motion (Left/Right or Up/Down) to pass the inclusion criterion. In the shape task, participants had to be able to discriminate between the two full-size (un-occluded) shapes, and understand the match-to-sample concept. To test this, several tests of increasing complexity were performed. The participants had to pass them all to qualify for the experiment. In the first test, the screen was divided into upper and lower halves. In each trial, one shape was shown alone in the upper screen half (i.e., sample) while both shapes appeared later together in the other half. The task was to report the matched shape. In the second test, one cross-like shape (the sample) moved across the screen (from top to bottom). Then, both the original image and its mirror-image shape appeared together, and the participant was required to choose the shape matching the previous sample. Finally, a number of slit-familiarization trials were presented (with the widest slit-width equal to 160% of the shape length, as above) to ensure that participants are able to recognize a sample shape when moving through a slit as well. In all cases subjects were required to have at least four consecutive correct answers to pass our criteria. All 23 cataract-treated participants qualified.

METHOD DETAILS

We used a 15'' laptop computer with a touch screen (resolution: 1366 × 768 pixels). The subjects sat at their preferred distance from the screen, typically 40 cm. This distance was kept constant across the tests, for each particular patient.

Experiment I

Initial tests on motion direction and cross-shape tasks

Twenty-three patients and fifty-one control participants completed the cross-shape task. Fifteen patients and thirty-two controls completed the motion-direction task (Table S1). The slit was either vertical or horizontal (in separate runs). Thus, the testing procedure included four different runs i.e., motion and shape assessment under vertical and horizontal slit orientation, which were presented in a counterbalanced order across participants.

In each trial, a simple shape (380 × 322 pixels, 9.45 × 8.0 cm, 13.47 × 11.42° at 40 cm distance) moved at a fixed speed (7.5 cm/s, 10.6°/s) in a direction orthogonal to the slit orientation, such that only a portion of the shape was visible at any instant (Figure 1A). The stimulus was a cross-like shape (constructed from identical ellipsoid elements) or its flipped version. It had a sufficient number of oriented contours to allow the perception of the shape motion within a slit. The cross-like shape was chosen, because below a critical slit-size (26.6% of the full image; Figures 2A and 2B, inserts), the slit-viewed shape could not be recognized by a local feature in the image: Shape recognition required temporal integration of the partial views.

In the motion-direction discrimination run, the task was to report the direction of slit-viewed motion (e.g., up or down for horizontal-slit trials). In the shape discrimination run, the cross-like shape (or its flipped counterpart) moved behind the slit, and participants were required to report the object's shape by pointing to/touching one of the two shapes (e.g., "upright" or "inverted" cross for horizontal-slit trials) that appeared immediately after the shape motion ended. In the test ("match") phase, the positions of the matching shape and its foil were randomly assigned, to avoid any spatial bias. In vertical-slit runs the computer screen was simply rotated by 90°. Correct responses were accompanied by a tone. Slit-width was adaptively changed (within the range 0.3 – 111% of the shape length) using a staircase procedure to assess the direction/shape discrimination threshold (in terms of slit-width). Each run ended when 8 reversals were registered or 48 trials were completed.

Sometimes, the run ended earlier due to fatigue, loss of interest or other reasons. The staircase was designed to minimize this problem, so that participants genuinely reach their threshold as fast as possible. To that end, the staircase procedure was structured in three phases: The initial trials followed one-down, one-up rule with a large step size (60 pix, 1.5 cm, 2° at 40 cm distance, 15.8% of the shape length). After the second error, a two-down, one-up rule was implemented, with smaller step size: 30 pixels (1°, 0.75 cm, 7.9% of the shape length). Note that although we changed the slit-size depending on performance right from the start, the error counting (necessary to move from phase I to phase II) began only after 8 trials were completed. Thus, the initial, accidental errors, had no effect on the individual's threshold. The final phase, using the three-down, one-up algorithm (with the finest step size, 10 pixels, 0.25 cm, 0.35°, 2.6% of the shape length) was implemented after the third counted error. If the slit-width reached 10 pixels, the next slit-width was 5, and changes were at increments of 1 pixel. The trials from phase III were exclusively used to assess the individual's threshold.

Recognition thresholds (at ~79%[27]) were calculated as the average of the final 8 reversals. Sometimes, the run ended prematurely before the maximum number of trials (n = 48) was reached. The minimal number of reversals for inclusion was 4. Patients reached six (or 8) reversals in 67% (62) of all tests (out of 92 tests on both shape and motion tasks & both slit orientations). In their two tests, the

Please cite this article in press as: Orlov et al., Learning to perceive shape from temporal integration following late emergence from blindness, Current Biology (2021), https://doi.org/10.1016/j.cub.2021.04.059

reversals were calculated after the second counted error (to pass the inclusion criterion). Two cross-shape tests were not included in the analysis (i.e., initial tests for p1 and p10 under vertical slit orientation, because they didn't pass our inclusion criterion). However, the performed trials (27 and 23, respectively) were accounted for as practice trials.

Re-test of the cross-shape task

Eleven patients participated in the multiple testing on the cross-shape task (Table S1). Five of them were re-tested on our cross-shape task a few (1-3) days after the first test. All eleven patients were re-tested on the same task approximately a year after the first test. As above, recognition thresholds were calculated as the average of the final reversals.

Image blur control

We also assessed the contrast sensitivity function (CSF) of each of the cataract-treated subjects (in both initial and latest tests, see Table S1 and Method details, Contrast sensitivity assessment for further details). The CSF cut-off frequency of the patient with the poorest visual acuity was 1.2 cpd (in the initial post-op test). To ensure that differences between the cataract-treated and control groups were not due to the patients' blurry vision, we prepared a low-pass filtered version of all the stimuli, and used them when testing the control participants: We took a conservative approach, eliminating all spatial frequencies above 1 cpd (Figure 1B). This was done by convolving each movie frame in the slit-viewing videos (as well as each image in the test presentation) with a 2D Gaussian blur kernel (σ (x) = 16 pixels i.e., 0.5° at 40 cm viewing distance, in both dimensions; the kernel size comprised of 3σ in both directions). Using a Gaussian kernel σ (x) = 0.5° corresponds to applying a Gaussian filter in the frequency domain where $\sigma(f) = (1/2\pi)/0.5° = 0.32$ cpd (given that $\sigma(x) * \sigma(f) = 1/2\pi$). After this, the power at 1cpd (our chosen cutoff frequency) is a mere 0.4% (−24 dB) of its original power (see also Figure S1D).

Alternative strategy to solve the cross-shape task

We chose simple cross-like shapes, made of identical elements, to eliminate (below a certain slit size) the possible use of specific local features for shape discrimination. However, this specific experimental design could not exclude the possibility that the task was performed by an assessment of two time intervals: (i) between the time of first appearance of the shape till the appearance of the orthogonal, elongated shape element, and (ii) from the time of disappearance of the orthogonal shape element, until the final disappearance of the whole shape. For example, when an upright cross moved up (in a horizontal-slit trial) the first interval was shorter than the second interval. When the cross was upside-down, the second interval was shorter. In our study, on each trial the object moved either up or down. Thus, to arrive at the correct decision without generating an internal image of object, both time intervals and the direction of motion had to be independently calculated, and then combined using complex logical operations. Still, since the same images were repeated, the newly-sighted patients may have had the opportunity to learn this strategy. The unique-shapes task was designed to test their temporal integration in conditions where this strategy was not useful.

Experiment II

Shape task using unique shapes

We tested twenty-one patients on another shape-integration task (Table S1) with a new set of trial-unique stimuli (having the same length as the cross-shape). While only one pair of images (with matched local features) was presented in the original cross-shape task, this new control task utilized 24 unique pairs (Figure 3). We used simple 2D stimuli. Their contours provided the only source of information about their shape. According to theoretical and behavioral studies,[28–30] information along a visual contour is concentrated in regions of high magnitude of curvature. Importantly, the shapes for each pair were created such that these regions, which actually represented the characteristic local visual features, were very similar between the shape pairs. Under slit-viewing conditions, this difference could not be detected, once the slit-width was smaller than the critical slit-width (Figure 3B, bottom), which was calculated for each pair comprising, on average, 30.4% of the full image (range across shapes: 25.0-38.9; SD = 4.5%). Note that we adopted a conservative measure, by taking the smaller threshold of the pair, as the critical integration criterion for each shape from the pair. Each image was shown traversing across the slit only once during the whole session. The only way to assess global shape with trial-unique stimuli, at slit-widths smaller than the critical value, was through an integration across time.

Specifically, on each trial, one of the shapes was shown moving behind a horizontal slit. Next, that shape was presented together with its *paired counterpart*, and as previously, the participants were asked to choose the image matching the one just seen moving behind the slit. As in the cross-shape task, slit-width was adaptively changed using a staircase procedure to assess the shape discrimination threshold (in terms of slit-width), and each run ended when 8 reversals were registered or 48 trials were completed. The initial trials followed one-down, one-up rule, while after the second error, a two-down, one-up rule was implemented till the end of the session. The error counting necessary to move across the experimental phases began after the first 6 trials. Twenty patients (out of 21 tested on this task) had at least 6 reversals (In five cases, we had to count reversals starting from the first error to pass this criterion). One patient had only four reversals.

The size of the staircase step was defined by the current slit-width (i.e., the narrower the current slit the smaller was the step). Specifically, slit sizes comprised of 440, 342, 266, 207, 163, 131, 111, 101, 92, 84, 76, 68, 60, 52, 44, 36, 28, 20, 12, 4 pixels (which was equal to 116, 90, 70, 54, 43, 34, 29, 27, 24, 22, 20, 18, 16, 14, 12, 9, 7, 5, 3, 1% of the shape length). Thus, the size of the staircase step was initially large (comprising roughly a quarter of the shape length) and decreased with narrowing the slit-width until the width reached the mean critical criterion for shape integration (~30% of the full image). After this, the slit size changed by 2% of the full shape length. The order of shape presentation was the following: Initially, all first exemplars from the 24 pairs ('left' exemplars in Figure 3A) were presented (in the corresponding trials) and then all second exemplars were shown (the order was randomized across participants). Shapes within each 24-shapes sequence were shown pseudo-randomly. Specifically, 24 shapes were divided into 4

Please cite this article in press as: Orlov et al., Learning to perceive shape from temporal integration following late emergence from blindness, Current Biology (2021), https://doi.org/10.1016/j.cub.2021.04.059

subgroups. The order of the subgroups' presentation was constant while the order within each subgroup was random (for each participant). This 'block' design allowed for randomization of shape presentation, while ensuring that overall, across subjects, the same shape pairs appear at roughly the same stages of the staircase.

Contrast sensitivity assessment

All patients completed this test several times after surgery [at the same (or adjacent) day as the main tests]. In each trial of the experiment, the participants saw a Gabor patch (19.4 cm in diameter) at a specific spatial frequency and contrast and were asked to report the grating orientation (horizontal or vertical). Their performance at the various contrast levels (per spatial frequency) was used to assess the contrast threshold at that frequency (for this purpose, the contrast was adaptively changed using a staircase procedure). Plotting the contrast threshold as a function of the spatial frequency yielded the CSF of the participant. The cutoff frequency, the highest spatial frequency that can still be seen by the viewer, was assessed by fitting the CSF with the truncated log-parabola form.[31] For more information about the CSF experiment see McKyton et al.[11]

The CSF of nineteen patients was also evaluated prior to surgery. However, in some newly-sighted participants, this was impossible due to either very poor visual acuity, lack of cooperation or unavailable testing procedures at that time. When the CSF test (based on the orientation discrimination task) was impossible/failed, it was replaced by a simpler (detection) test. In this test, a large white circle was shown on a black background, at varying spatial positions. Participants were asked to detect and touch the circle. Its size was adaptively changed using a staircase procedure to assess the threshold circle size for detection. Next, when possible, the circle was replaced by a two-cycle Gabor patch (at full contrast), whose size and position was changed using the same staircase procedure, to assess the highest possible spatial frequency, at which detection was still possible. This was used as an estimation of the cutoff frequency. The preferred distance (from the screen) of patients in the pre-op acuity testing was 5-40 cm.

Stimulus Presentation

Stimuli presentation was controlled by Presentation software (Neurobehavioral Systems USA, Version 22).

QUANTIFICATION AND STATISTICAL ANALYSIS

In both experiments, a staircase procedure was used to assess the shape or motion discrimination threshold in terms of slit-width (see Method details).

Experiment I

Normalization of the cross-shape recognition threshold

The individual's recognition threshold was normalized by the critical slit-width for that task (26.6% of the shape length), by taking the log of their ratio.

Experiment II

Normalization of the unique-shapes recognition threshold

The stimuli differed in their critical criterion for shape integration (see Method details, Experiment II). Note that stimuli with larger critical slit-width were the more difficult ones: they required obligatory use of temporal integration strategy at an earlier stage of the staircase, when stimuli with smaller critical slit-width could still be discerned based on local cues. Furthermore, the number of completed trials differed between the patients due to loss of interest, etc. (range: 22 – 48 trials; mean = 36 trials; SD = 8). Thus, the actual stimuli seen by the patients were not always exactly the same.

This variation, between stimuli and individuals, is likely to cause biases if unaccounted for. To address this issue, we calculated the normalized threshold in the unique-shapes task per trial, by considering the specific shape viewed on that trial. Specifically, we normalized the recognition threshold of each trial by the corresponding critical slit-width for the shape pair to which that specific shape belongs (i.e., taking the log of their ratio, see also Method details, Experiment II). Eventually, each individual's recognition threshold was assessed by computing the average across the final 6 reversals using their normalized values. Given the variation in the critical slit-width across stimuli, it may actually be more useful to calculate the individual threshold by averaging all normalized slit values at the staircase asymptote (starting from the first reversal [out of the six final reversals]). This resulted in very similar results to the conventional method (for details, see Figure S3K).

Accounting for previous experience with the cross-shape task

The patients tested on the unique-shapes task were divided into two groups: (i) a ''practiced'' subgroup, with previous experience on the *cross*-shape test at least 6 months earlier (range 87-276 trials; mean = 192 trials; SD = 78) so that the learned skill had already been consolidated in memory[32] and (ii) the ''naïve'' patients, which had only 45 cross-shape trials on the same day, just before the unique-shapes test (range: 39 – 48 trials; SD = 4). Importantly, the two subgroups (''naive'' and ''practiced'') did not differ in their level of cross-shapes discrimination performance in their *initial* test (horizontal-slit trials: $t(19) = 0.33$, $p = 0.748$; both horizontal- and vertical-slit trials: $t(19) = 0.77$, $p = 0.450$). This indicates that the ''practiced'' subgroup was *not* better than the ''naïve'' subgroup, *a priori*, due to sheer coincidence. We conclude that the superior performance of the ''practiced'' subgroup in the novel unique-shapes task was indeed due to their previous practice in the cross-shapes task.

Please cite this article in press as: Orlov et al., Learning to perceive shape from temporal integration following late emergence from blindness, Current Biology (2021), https://doi.org/10.1016/j.cub.2021.04.059

Statistics

Behavioral data were processed and analyzed using MATLAB R2019b (version 9.7.0, Mathworks, Natick, MA). Subsequent statistical analyses were performed using MATLAB and SPSS (version 26.0, SPSS, Chicago, IL).

Experiment I

We applied a multi-factorial repeated-measures ANOVA to analyze thresholds for motion and shape discrimination in 11 (out of 23) patients (p2-9 and p11,12,14 in Table S1) and 17(out of 51) controls, who completed both cross-shape and motion-direction tasks under both slit orientations. Within-subjects factors were slit orientation (horizontal, vertical) and task (direction, shape), while the between-subjects factor was the group identity (patients, controls). Follow-up post hoc t tests were also performed. We also examined whether the shape recognition thresholds (averaged across slit orientation) were below the critical slit size in both patient and control groups, and if there was any difference between the groups, using two-sided t tests.

To quantify the effect of practice in 11 patients following their multiple testing on the cross-shape task (p1-11 in Table S1), we applied a linear mixed model on all observations, with the fixed test-repetition factor (the levels were: $1^{st,}$ 2^{nd} and 3^{rd} test). Visual acuity (i.e., the cutoff spatial frequency transformed to log units) was added as a covariate. In addition, we used two-sided t test to compare the patients' performance in the initial and the latest cross-shape tests.

The analyses of variance were performed on log-transformed data (i.e., the threshold slit-width as percent of the shape length in log units) to meet the required normal distribution assumptions of the models' residuals. The t tests were also calculated using the log-transformed data.

Experiment II

We tested the effect of previous experience with the cross-shape recognition on the unique-shapes performance, in 21 patients, who performed both shape tasks (p1-10 and p13-23). To that end, we used multi-factorial ANOVA. The dependent variable was the recognition threshold in the unique-shapes task (normalized as explained in Quantification and statistical analysis, Experiment II). The factor of interest was previous practice (with the two levels, practiced and naive). Visual acuity and time since surgery served as covariates. Specifically, the 'practiced' subgroup included twelve patients: p1-10, p13 and p14; The nine 'naive' patients were p15-23 (Table S1). We also assessed the Pearson correlation coefficient between the normalized cross-shape recognition thresholds and the unique-shapes performance (in the horizontal slit orientation used in both tests).

For ANOVAs, η_p^2 was computed as a measure of effect size. Cohen's d was computed as a measure of effect size for the t test, which compared the patients' performance in the initial and the latest cross-shape tests. For Pearson correlations, Pearson's r was the measure of effect size.